MOR-004 第3相試験

- BMN110の安全性と有効性の評価
- ムコ多糖症ⅣA型(モルキオA症候群)
- 3群で検討
  プラセボ投与群
  BMN110 2mg/kg 毎週投与群
  BMN110 2mg/kg 隔週投与群
- 主要評価項目
  6分間歩行距離の増加
- 副次的評価項目
  3分間昇段テスト
  尿中ケラタン硫酸(KS)の減少

図3 ムコ多糖症Ⅳ A型に対する酵素補充療法製剤 BMN 110の国際共同治験 MOR004の概要
MOR004は，BMN11の第3相試験で，日本，韓国，台湾などアジア諸国を加えた国際共同治験として行われた．小児希少疾患治療薬の国際共同治験に参加した例としては，国内初の治験である．

数とその年齢分布等の疫学的情報を強く求められた．これは，製薬企業として必要なマーケットリサーチに相当する貴重な情報であるが，製薬企業のみでは入手することが困難な情報でもある．MOR004の治験参加が実現したことは，治療薬開発を推進するうえで，超希少疾患の臨床情報データベースを体系的に整備することの重要性を示唆している．日本先天代謝異常学会では，21の患者家族会の協力の下に，患者登録と超希少疾患のデータベース作成を進めている（図4）．

治験デザインの検討

超希少疾患の治験は，「対象患者数が十分に得られない」状況で行われる．その中で，臨床的にも明らかな有効性を示すことは，困難な場合が少なくない．特に，精神運動発達遅滞の予防につながるような薬剤においては，発達評価を指標とする治験が必要になるが，短期間で発達について有

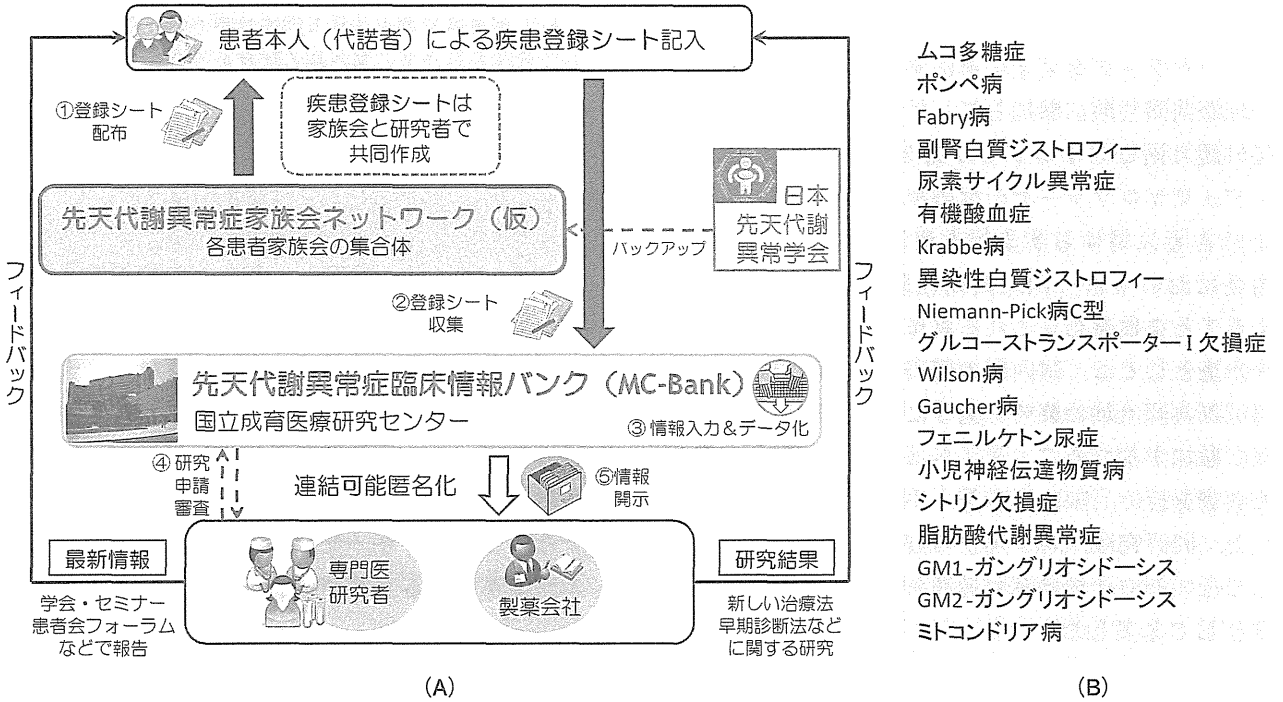

図4 先天代謝異常症患者登録フォローアップシステムの概要
患者家族会を主体とした先天代謝異常症の臨床情報データベースの構築とその臨床研究や治験への活用法を示す（A）．対象疾患は，現在19疾患におよぶ（B）．

効性を評価することは困難である．そのような場合，適切なバイオマーカーの推移を主要評価項目とするなど，サロゲートエンドポイントの活用も必要となろう

結　　語

小児希少疾患治療薬の臨床開発の諸問題について検討した．特に，ドラッグラグ解消のためには，国際共同治験に日本が積極的に参加することが不可欠であること，患者登録と超希少疾患のデータベース作成の必要性について述べた．

文　　献

1）Okuyama T, Tanaka A, Suzuki Y, Ida H, Tanaka T, Cox GF, Eto Y and Orii T. Japan Elaprase® Treatment (JET) study: Idursulfase enzyme replacement therapy in adult patients with attenuated Hunter syndrome (Mucopolysaccharidosis II, MPS II). Mol Genet Metab. 2010; 99: 18-25.

2）鈴木康之．ムコ多糖症Ⅳ型に対する疫学調査：厚生労働科学研究補助金（医療技術実用化総合研究事業）「新規治療法が開発された小児希少難病の疫学調査と長期フォローアップ体制の確立に関する研究」（研究代表者：奥山虎之）平成22年研究報告書11-13.

NEUROPATHOLOGY

Neuropathology 2014; **34**, 49–57 doi:10.1111/neup.12047

Case Report

Niemann-Pick disease type C1 predominantly involving the frontotemporal region, with cortical and brainstem Lewy bodies: An autopsy case

Yoichi Chiba,[1] Hiraku Komori,[2] Shiro Takei,[1,5] Sanae Hasegawa-Ishii,[1,6] Noriko Kawamura,[1] Kaori Adachi,[7] Eiji Nanba,[7] Masanori Hosokawa,[1] Yasushi Enokido,[1] Zen Kouchi,[1] Futoshi Yoshida[3] and Atsuyoshi Shimada[1,4]

[1]Department of Pathology, Institute for Developmental Research, [2]Kobato Gakuen, Aichi Human Service Center, Departments of [3]Internal Medicine, [4]Pathology and Laboratory Medicine and Radiologic Technology, Central Hospital, Aichi Human Service Center, Kasugai, [5]Faculty of Nutrition, Koshien University, Takarazuka, [6]Japan Society for the Promotion of Science, Tokyo, and [7]Division of Functional Genomics, Research Center for Bioscience and Technology, Tottori University, Yonago, Japan

Niemann-Pick disease type C (NPC) is an autosomal recessive neurovisceral lipid storage disorder. Two disease-causing genes (*NPC1* and *NPC2*) have been identified. NPC is characterized by neuronal and glial lipid storage and NFTs. Here, we report a man with juvenile-onset progressive neurological deficits, including pyramidal signs, ataxia, bulbar palsy, vertical supranuclear ophthalmoplegia, and psychiatric symptoms; death occurred at age 37 before definitive clinical diagnosis. Post mortem gross examination revealed a unique distribution of brain atrophy, predominantly in the frontal and temporal lobes. Microscopically, lipid storage in neurons and widely distributed NFTs were observed. Lipid storage cells appeared in systemic organs and filipin staining indicated intracellular cholesterol accumulation in hepatic macrophages. Electron microscopy revealed accumulation of lipids and characteristic oligolamellar inclusions. These findings suggested an NPC diagnosis. Neuronal loss and gliosis were frequently accompanied by NFTs and occurred in the frontal and temporal cortices, hippocampus, amygdala, basal forebrain, basal ganglia, thalamus, substantia nigra and brain stem nuclei. Lewy bodies (LBs) were observed in most, but not all, regions where NFTs were evident. In contrast, neuronal lipid storage occurred in more widespread areas, including the parietal and occipital cortices where neurodegeneration with either NFTs or LBs was minimal. Molecular genetic analysis demonstrated that the patient had compound heterozygous mutations in the cysteine-rich loop (A1017T and Y1088C) of the *NPC1* gene. To our knowledge there has been no previous report of the A1017T mutation. The pathological features of this patient support the notion that NPC has an aspect of α-synucleinopathy, and long-term survivors of NPC may develop a frontotemporal-predominant distribution of brain atrophy.

Key words: frontotemporal atrophy, Lewy body, neurofibrillary tangle, Niemann-Pick disease type C, *NPC1* gene.

INTRODUCTION

Niemann-Pick disease type C (NPC, MIM 257220) is an autosomal recessive neurovisceral lysosomal lipid storage disorder characterized by abnormal intracellular trafficking of endocytosed cholesterol with sequestration of unesterified cholesterol and glycolipids in the endosomal/lysosomal system.[1,2] NPC is caused by mutations in either the *NPC1* (95% of cases) or *NPC2* gene.

NPC is neuropathologically characterized by the combination of abnormal lysosomal storage in neurons and glia and the presence of NFTs.[3,4] In contrast to relatively constant microscopic features, the distribution of gross brain atrophy varies among cases: some patients develop frontal atrophy, others exhibit pronounced brainstem and cerebellar atrophy, and still others have no obvious gross abnormalities.[2,3,5]

In addition to NFTs, Saito *et al.* reported accumulation of phosphorylated α-synuclein in NPC patients with *NPC1*

Correspondence: Atsuyoshi Shimada, MD, PhD, Department of Pathology, Laboratory Medicine and Radiologic Technology, Central Hospital, Aichi Human Service Center, 713-8 Kamiya, Kasugai, Aichi 480-0392, Japan. Email: ats7@inst-hsc.jp

Received 6 December 2012; revised and accepted 2 May 2013; published online 27 May 2013.

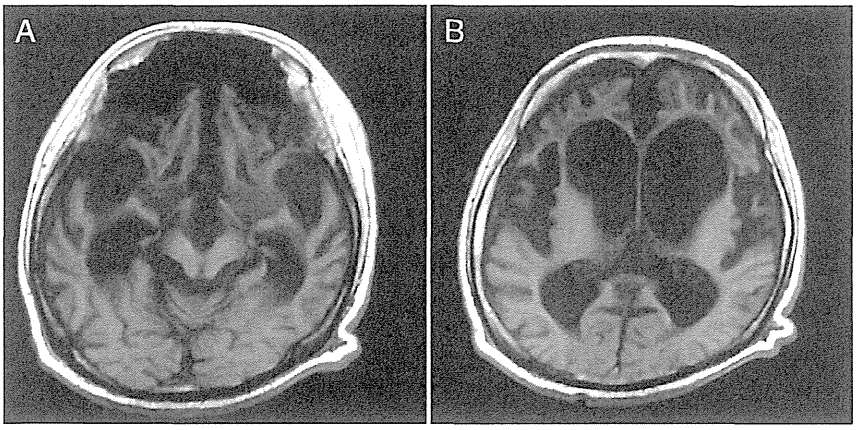

Fig. 1 T1-weighted MRI at 31 years of age. (a) Marked atrophy in the brainstem, cerebellum, hippocampus and (a and b) frontotemporal lobes is observed. Note relative sparing of the parietooccipital region compared to the frontotemporal region.

mutations and suggested that NPC could be categorized as an α-synucleinopathy.[6] However, cortical and brainstem-type Lewy bodies (LBs) were observed in only two of 12 cases examined,[6] and to our knowledge few other investigators have described accumulation of α-synuclein in NPC brains.

Here, we report an autopsy case of juvenile-onset NPC with marked brain atrophy that predominantly affected the frontal and temporal lobes. In addition, the concurrence of LBs in the cerebral cortices and brainstem was found in this patient. Molecular genetic analysis revealed compound heterozygous mutations of the *NPC1* gene, one of which is a missense mutation in the cysteine-rich loop that to our knowledge has not previously been reported.

Clinical summary

The patient was a 37-year-old man with no family history of neurological diseases or consanguineous marriage. His parents first noticed learning difficulties and a gait disturbance at 8 years of age. During the following several years, there was progressive deterioration of verbal communication, memory and fine motor control of fingers. He also developed dysphagia, fecal incontinence, problems in social interaction/behavior, and grand mal seizures. At 11 years of age, neurological examination revealed bilateral pyramidal signs in the lower extremities, truncal and limb ataxia, vertical supranuclear ophthalmoplegia, dysarthria and dysphagia. Computed tomography revealed atrophy in the cerebrum, brainstem and cerebellum. Electroencephalography (EEG) revealed bilateral frontal sharp waves. Electromyography, nerve conduction studies, and serum and urinary amino acid analysis were unremarkable. Analysis of CSF revealed mild elevation of IgG (7.5 mg/dL). Bone marrow examination was inconclusive. Activities of sphingomyelinase and hexosaminidase were within normal limits. Abdominal ultrasonography was negative for hepatosplenomegaly, as it was during the entire course of the illness. By the age of 14 years, the patient had become tetraparetic. A gastrostomy tube was placed because of increasing dysphagia at 16 years of age. He subsequently became bedridden with total dependence. At age 22, a tracheostomy was performed and respiratory support with mechanical ventilation was started. Brain MRI performed at 31 years of age revealed marked brain atrophy, especially in the frontotemporal lobes, hippocampus, brainstem and cerebellum (Fig. 1). In contrast to severe involvement of the frontotemporal region, the parieto-occipital region was relatively spared (Fig. 1). Seizures were well-controlled by phenobarbital and carbamazepine, and no apparent episodes occurred during the last 12 years of his life. The last EEG was performed at age 31 and showed no epileptic discharge. He died from acute pancreatitis at age 37 years. The clinical diagnosis at the time of death was unclassified neurodegenerative disease of childhood onset.

METHODS

Pathological examination and immunohistochemistry

An autopsy was performed 3 h after death. All organs were fixed with 10% phosphate-buffered formalin. Paraffin-embedded tissue blocks were cut into 6 μm sections, which were then stained with HE. CNS tissue sections were subjected to KB staining. The Gallyas-Braak silver stain and immunohistochemistry were performed on selected CNS sections.

For filipin staining, liver tissue was embedded in O.C.T. compound (Sakura Finetechnical Co., Tokyo, Japan) and cryosections of 10 μm thickness were cut using a Bright OTF Cryostat (Bright Instrument Co. Ltd, Huntingdon, UK). Sections were immersed in 10% phosphate-buffered formalin for 10 min at 4°C, washed with distilled water three times, and incubated with 0.1 mg/mL filipin III

(Cayman Chemical, Ann Arbor, MI, USA) for 1 h at room temperature in the dark. After rinsing in PBS, sections were coverslipped using a SlowFade Antifade kit (Invitrogen Life Technologies Corp., Carlsbad, CA, USA) and fluorescent images were acquired using a fluorescent microscope (Axiovert 200 M, Carl Zeiss Co. Ltd, Oberkochen, Germany).

Antibodies used for immunohistochemical analyses included anti-ubiquitin (rabbit polyclonal, 1:1000, DakoCytomation, Glostrup, Denmark and mouse monoclonal, 1:1000, Merck Millipore, Billerica, MA, USA), anti-phosphorylated tau (AT8; mouse monoclonal, 1:1000, Innogenetics, Gent, Belgium), anti-α-synuclein (4D6; mouse monoclonal, 1:1000, GeneTex, Irvine, CA, USA), anti-histone deacetylase (HDAC) 6 (H-300; rabbit polyclonal, 1:200, Santa Cruz Biotechnology, Santa Cruz, CA, USA), anti-p62/sequestosome 1 (p62/SQSTM1) (rabbit polyclonal, 1:1000, Medical & Biological Laboratories, Nagoya, Japan), and anti-apolipoprotein E4 (ApoE4) (mouse monoclonal, 1:100, Medical & Biological Laboratories). Tissue sections were deparaffinized and pretreated with 0.3% hydrogen peroxide in methanol for 30 min at room temperature to block endogenous peroxidase activity. For staining with anti-p62/SQSTM1 antibody, antigens were retrieved by heating sections at 80°C in 10 mmol/L citrate buffer, pH 6.0, for 3 h prior to the hydrogen peroxide treatment. After non-specific binding was blocked with 10% normal goat serum (NGS), sections were incubated with primary antibodies at 4°C overnight. All antibodies were diluted in 10% NGS. Sections were washed in PBS and then incubated with secondary anti-rabbit or anti-mouse IgG antibodies conjugated to horseradish peroxidase (Envision+ System, DakoCytomation) at room temperature for 1 h. Reactions were visualized with 0.4 mg/mL 3,3′-diaminobenzidine (DAB) in PBS containing 0.006% H_2O_2 for 10 min. Nuclei were counterstained with hematoxylin.

Electron microscopy

Transmission electron microscopy was performed as previously described.[7] Formalin-fixed specimens were dissected into 1 mm^3 pieces, and were then post-fixed with 2.5% glutaraldehyde in 0.1 mol/L phosphate buffer (PB; pH 7.4) for 4 h and 1% OsO_4 in PB at 4°C for 1 h. Specimens were dehydrated using a graded series of alcohols and QY-1 (Nisshin EM Co., Ltd, Tokyo, Japan), and then embedded in Quetol 812 (Nisshin EM). Ultrathin sections were cut with an LKB ultramicrotome (LKB-Produkter, Bromma, Sweden), and sections were counterstained with aqueous TI-blue (Nisshin EM) and Sato's lead citrate.[8] Sections were examined using a 1200EX transmission electron microscope (JEOL Ltd, Tokyo, Japan).

NPC1 gene mutation analysis

Written informed consent was obtained from the patient's parents for the genomic analysis and for publication of the results. Genomic DNA was extracted from frozen liver and spleen using standard protocols. PCR primers were designed to amplify all the exons of *NPC1* and flanking intron regions. Direct sequencing of PCR products was performed using a 3130xl genetic analyzer (Applied Biosystems, Foster City, CA, USA), and sequence data were analyzed as previously described.[9]

RESULTS

Pathological findings

At autopsy, the spleen weighed 169 g, slightly heavier than usual. The liver weighed 1058 g and hepatomegaly was not apparent. The pancreas was hemorrhagic in the head, body and tail, indicative of acute hemorrhagic pancreatitis.

The brain weight was 731 g. Gross neuropathological findings included marked atrophy of the frontal and temporal lobes bilaterally (Fig. 2a), cerebellum, brainstem and spinal cord. Coronal sections of the cerebrum exhibited marked atrophy of the deep white matter with thinning of the corpus callosum, marked atrophy of the frontal and temporal cortices and mild to moderate atrophy of the parietal and occipital cortices. Atrophy was also marked in the amygdala, hippocampi, parahippocampal regions, thalamus and hypothalamus, and was accompanied by dilatation of the lateral and third ventricles (Fig. 2b). The Sommer's sectors of hippocampi bilaterally exhibited brownish discoloration (Fig. 2b). The superior temporal gyri were relatively spared compared with the middle and inferior temporal gyri (Fig. 2b). The substantia nigra and locus ceruleus were depigmented.

Histopathological examination revealed marked neuronal loss and gliosis in widespread areas, including the frontal and temporal cortices, hippocampi and parahippocampal regions, amygdala, thalamus, hypothalamus, midbrain and cerebellar cortex. Degeneration was advanced to form laminar necrosis-like changes in the middle layers of the frontal and temporal cortices (Fig. 3a). Numerous swollen storage neurons were present throughout the CNS (Fig. 3b). NFTs were frequently found in the CNS regions where neuronal loss and gliosis were prominent, such as the frontal and temporal cortices, hippocampus, amygdala, hypothalamus, basal ganglia, thalamus, brainstem and spinal cord (Fig. 3c,d). These findings strongly suggested the diagnosis of NPC.

Histopathological findings outside the CNS included the occurrence of lipid-laden foamy macrophages in the bone marrow, spleen (Fig. 4a), liver (Fig. 4b) and lung. Filipin staining of the liver sections revealed that Kupffer

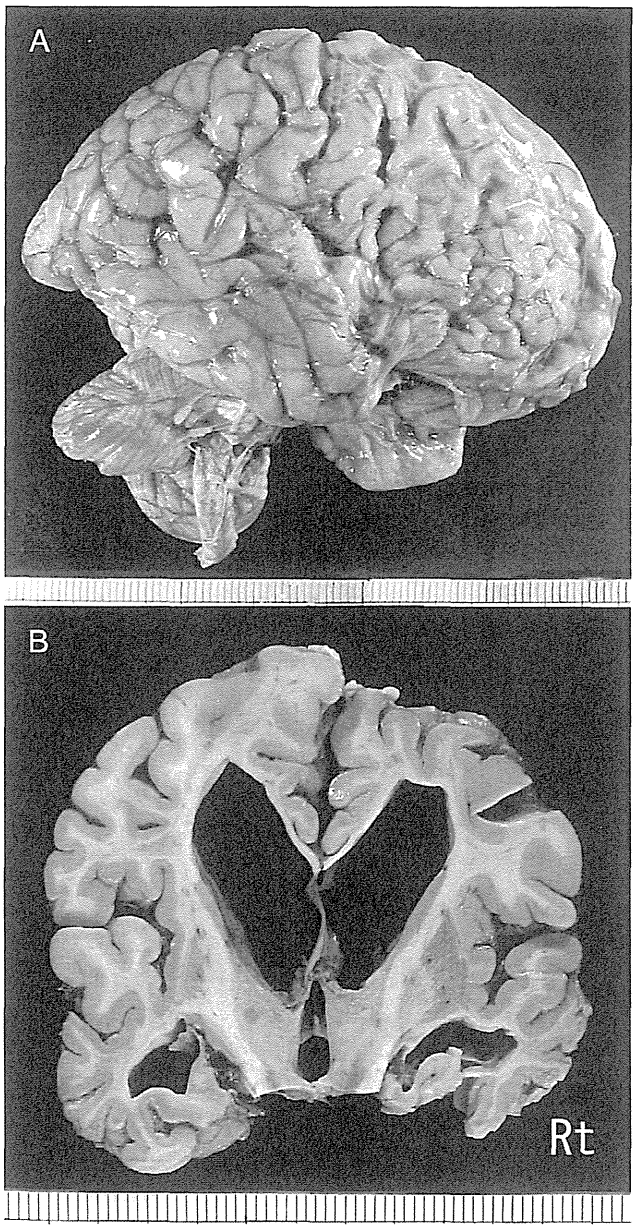

Fig. 2 Gross neuropathological findings. (a) Lateral aspect of the brain. Note marked atrophy of the frontal and temporal lobes. (b) Coronal sections of the cerebral hemisphere exhibited marked atrophy of the deep white matter with thinning of the corpus callosum, atrophy of the frontal and temporal cortices, hippocampus, parahippocampal region, thalamus and hypothalamus, accompanied by dilatation of the lateral and third ventricles. The Sommer's sectors of hippocampi bilaterally exhibited brownish discoloration. The superior temporal gyri were relatively spared compared with the middle and inferior temporal gyri.

cells (sinusoidal macrophages) accumulated intracellular free cholesterol (Fig. 4c). Ultrastructural examination revealed accumulation of electron-dense materials in liver macrophages (Fig. 5a) and membrane-bound oligolamellar inclusions typical of NPC in the occipital cortex (Fig. 5b, arrows).

In addition to the above-mentioned findings, which have been well recognized as characteristic of NPC, LBs were observed in many CNS regions. In HE-stained sections, LBs presented as eosinophilic hyaline masses against a background of accumulated lipids in swollen storage neurons (Fig. 6a,b). Cortical LBs were also found in some neurons with minimal lipid storage (Fig. 6c). LBs were distributed mainly in deeper layers of the cortices of the frontal and temporal lobes, especially the anterior cingulate cortex, as well as the subiculum, amygdala, basal forebrain, hypothalamus, substantia nigra, oculomotor nucleus, superior colliculus, locus ceruleus, inferior olivary nucleus, and dorsal motor nucleus of the vagus nerve. LBs were immunohistochemically stained for α-synuclein and ubiquitin, as well as for HDAC6 and p62/SQSTM1, both of which are known to localize in LBs of Parkinson's disease and dementia with LBs (Fig. 6d–g).[10,11] The distribution of swollen storage neurons, NFTs and LBs is summarized in Table 1.

Immunohistochemical staining with anti-ApoE4 antibody revealed no immunoreactivity in the brain, suggesting that this patient did not have the ApoE ε4 allele (data not shown).

Genetic analysis

Analysis of the *NPC1* gene revealed that the patient was a compound heterozygote for a G > A transition at cDNA nucleotide 3049, which is predicted to cause an alanine to threonine substitution in exon 21 at codon 1017 (A1017T), and an A > G transition at cDNA nucleotide 3263, which is predicted to cause a tyrosine to cysteine substitution in exon 22 at codon 1088 (Y1088C). To the best of our knowledge, the former mutation (A1017T) has not previously been reported.

DISCUSSION

To make a clinical diagnosis of NPC is often difficult, as in the present case, due to the extreme clinical heterogeneity of the disease: there is a wide range in the age of onset (ranging from the perinatal period to late adulthood), survival time (ranging from days to more than 60 years), and initial manifestations (including hepatic, pulmonary, neurological and psychiatric abnormalities).[2,5] This diversity of clinical presentation may cause significant diagnostic delay.[5,12–14] The absence of organomegaly in the present patient caused further difficulties for assignment of a clinical diagnosis of NPC; only 10% of juvenile-onset, but 50% of adult-onset, NPC patients lack hepatosplenomegaly.[2,5]

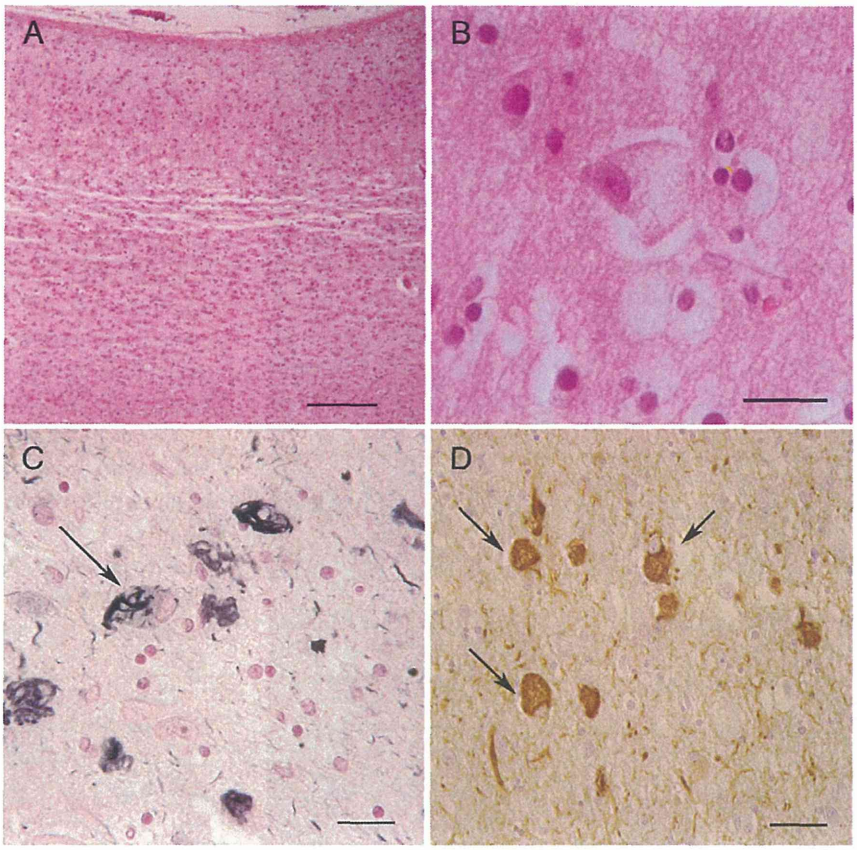

Fig. 3 Microscopic neuropathological findings. (a) Severe neuronal loss and gliosis of the cortex of the medial aspect of the precentral gyrus. Advanced degeneration with a laminar necrosis-like appearance was evident in the middle layers of the cortex. HE stain. (b) Swollen storage neurons distended with accumulated lipids in the cortex of the medial aspect of the precentral gyrus. HE stain. NFTs were frequently seen in the (c) CA1 pyramidal cells (Gallyas-Braak silver stain) and (d) neurons of the frontal cortex (AT8 immunohistochemistry). Storage neurons often contained NFTs (arrows). Bars: (a) 200 μm; (b–d) 20 μm.

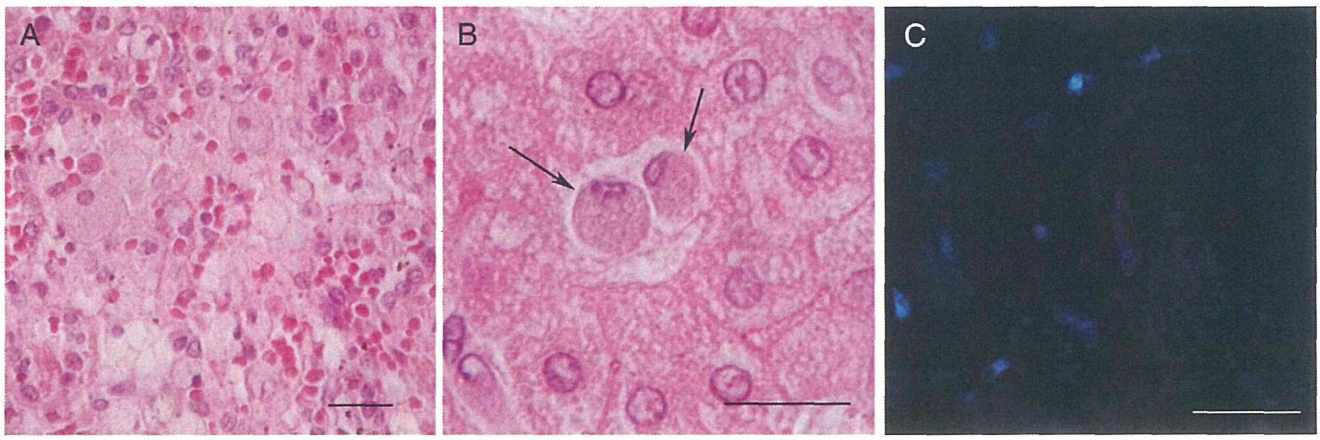

Fig. 4 Histopathological findings outside the central nervous system. (a) Numerous lipid-laden foamy macrophages in the splenic pulp. HE stain. (b) Lipid-laden Kuppfer cells were frequently seen in the hepatic sinusoids (arrows). HE stain. (c) Intracellular free cholesterol in Kuppfer cells was detected by filipin staining. Bars: (a, b) 20 μm; (c) 50 μm.

However, when we retrospectively reviewed the clinical features of this patient, we could have considered the possibility of NPC, based on the concurrence of childhood-onset ataxia and vertical supranuclear ophthalmoplegia. Early diagnosis is important, since miglustat has proven to be effective for treatment of progressive neurological changes in NPC patients.[2]

Predominantly frontotemporal atrophy was a unique feature of the present case. Some investigators have previously reported frontal atrophy in some NPC cases as evidenced by clinical imaging. MRI and positron emission tomography have revealed frontal lobe atrophy in some patients, especially in those with predominant psychiatric or cognitive symptoms.[5,14–16] Other investigators have

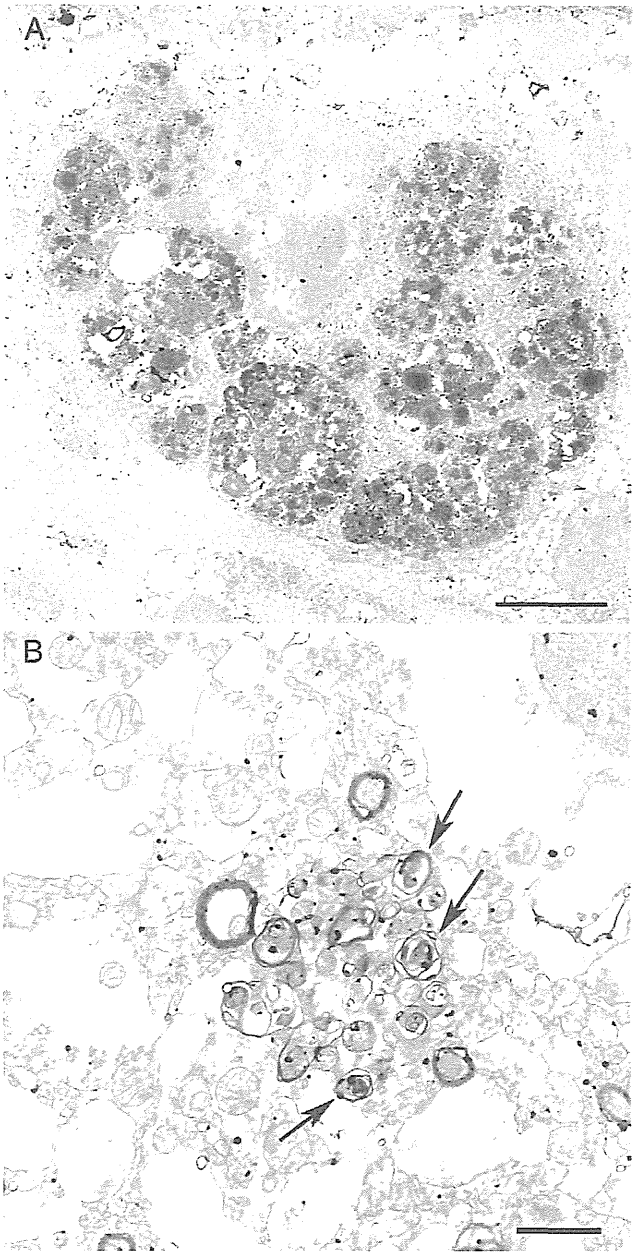

Fig. 5 Ultrastructural examination. (a) Cytoplasm of a liver macrophage was filled with electron-dense material, consistent with lipid accumulation. (b) Cytoplasmic membrane-bound oligolamellar inclusions were evident in the occipital cortex (arrows). Bars: (a) 2 μm; (b) 1 μm.

reported pathologically confirmed frontal lobe atrophy in NPC cases.[3,17] Klünemann *et al.* reported an autopsy case of adult-onset NPC due to a mutation of HE1/NPC2, exhibiting frontal lobe atrophy and lysosomal storage virtually restricted to neurons.[17] Histopathological analysis has previously revealed that NFTs were more intensely distributed in the frontal lobe than in the occipital lobe in NPC,[3] suggesting that the disease process predominantly affected the frontal brain areas. Although an MRI volumetric study has revealed partial reductions in the temporal lobe gray matter volume, such as of the planum temporale, Heschl gyrus, hippocampus and parahippocampal gyrus,[18] involvement of the entire temporal lobe in NPC has not previously been described, to our knowledge. Involvement of almost the entire temporal lobe, as in the present case, may be a manifestation of the end-stage of the disease course.

The formation of LBs in various cortical regions and brainstem nuclei is another conspicuous feature of the present patient, which supports the previously reported notion of NPC as an α-synucleinopathy.[6] The interactions between tau and α-synuclein may promote their assembly, as has been suggested.[19,20] Thus, accumulation of tau may enhance the aggregation of α-synuclein to form LBs. The ApoE ε4 allele has also been reported to enhance the accumulation of both tau and α-synuclein,[6,21] although our patient did not have the ApoE ε4 allele (data not shown). It is noteworthy that the accumulation of α-synuclein is a common feature of several human lipidoses, including Gaucher disease[22] and GM2 gangliosidosis.[23] Although the intracellular accumulation of unesterified cholesterol is a feature of NPC,[1,2] cholesterol accumulation in neurons has been reported to be minimal.[24,25] Instead, the secondary accumulation of glycolipids such as GM2 and GM3 ganglioside, lactosylceramide and glucosylceramide has been evident in NPC brains.[25–28] Findings of specific glycolipid accumulation in lipidoses accompanied by α-synuclein pathology suggest that there may be some specific relationship between neuronal storage of certain glycolipids and α-synuclein accumulation.

In the present case, brain regions with a relatively heavy NFT burden exhibited relatively severe neuronal loss and gliosis. Although some discrepancy was seen in the hippocampus, basal ganglia and thalamus, the distributions of NFTs and LBs were similar, particularly in the cerebral cortex, in our patient (Table 1), which is consistent with a previous report.[6] In contrast, in the present case, the distribution of swollen storage neurons in the cerebral cortex was different from that of NFTs, in that swollen storage neurons were frequently present even in the parietal and occipital cortices with relatively few NFTs. Thus, neuronal lipid storage may not directly lead to neurodegeneration.

Genetic analysis revealed that our patient had compound heterozygous mutations in the *NPC1* gene. Mutation of exon 22 (Y1088C) has previously been reported,[12,29] whereas that of exon 21 (A1017T) has not been described, to our knowledge. Both mutations cause amino acid substitutions in the cysteine-rich loop,[30] which has been suggested to be important for cholesterol trafficking by the NPC1 protein.[31] This domain harbors about one-third of the described *NPC1* mutations.[2] Since cultured fibroblasts were not obtained from our patient, the biochemical

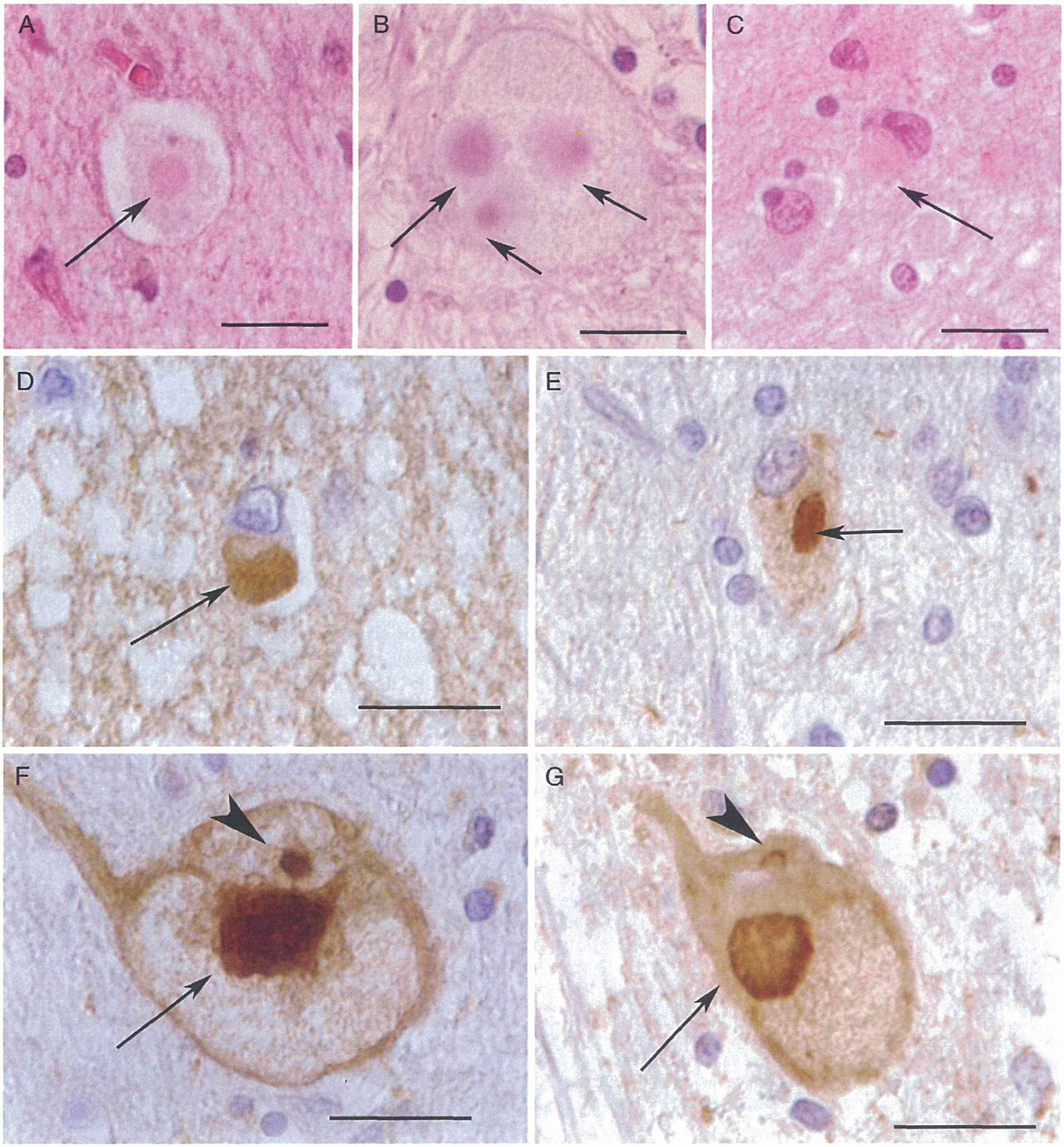

Fig. 6 Occurrence of Lewy bodies (LBs) in the cerebral cortex and brainstem. (a) A cortical LB (arrow) formed in lipid-filled cytoplasm of a neuron in the frontal cortex. HE stain. (b) LBs (arrows) in a swollen storage cell of the midbrain. HE stain. (c) Cortical LB (arrow) in an amygdala neuron with minimal lipid storage. HE stain. (d–g) LBs (arrows) were immunohistochemically stained for (d, frontal cortex) α-synuclein, (e, frontal cortex) ubiquitin, (f, midbrain) HDAC6 and (g, midbrain) p62/SQSTM1. (f and g, arrowheads) Marinesco bodies were also immunohistochemically stained with anti-HDAC6 and anti-p62/SQSTM1 antibodies. Bars: 20 μm.

Table 1 Distribution and severity of histological findings

	Swollen storage neurons	NFTs	LBs
Frontal cortex	3†	3‡	3§
Anterior cingulated cortex	3	3	3
Temporal cortex	3	3	2
Parietal cortex	3	1	1
Occipital cortex	3	0	1
Dentate gyrus	2	3	0
Cornus ammonis	3	3	0
Subiculum	3	3	3
Parahippocampal gyrus	3	3	3
Amygdala	3	3	3
Caudate/putamen	2	2	0
Globus pallidus	3	2	0
Basal forebrain	3	3	2
Thalamus	3	3	1
Subthalamic nucleus	3	3	2
Hypothalamus	2	3	2
Substantia nigra	3	2	3
Oculomotor nucleus	3	2	2
Superior colliculus	3	3	3
Locus ceruleus	3	3	3
Pontine nucleus	2	1	1
Inferior olivary nucleus	2	2	2
Dorsal motor nucleus of the vagus nerve	3	3	2
Hypoglossal nucleus	3	2	1
Cerebellar cortex	1	0	0
Dentate nucleus	2	1	0
Spinal cord	2	2	1

LB, Lewy body; NFT, neurofibrillary tangle. †Swollen storage neurons: 1, less than 25% of neurons have lipid storage; 2, 25–50% of neurons have lipid storage; 3, more than 50% of neurons have lipid storage. ‡NFT: 0, none; 1, 1–3 NFTs/high power field (hpf; visual field under a 40× objective lens); 2, 4–9 NFTs/ hpf; 3, 10 or more NFTs/ hpf. §LB: 0, none; 1, 1 or less LBs/low power field (lpf; visual field under a 10× objective lens); 2, 2–4 LBs/ lpf; 3, 5 or more LBs/ lpf. The result from an average of 10 visual fields was used for semiquantitative grading.

phenotype of this newly identified mutant protein was not determined. Instead, we plan to perform experiments using animal cell cultures to determine the functional significance of the mutation of exon 21 (A1017T). Further analyses of NPC1 would contribute to more detailed elucidation of the function of this protein, which could lead to better understanding of this devastating disease.

ACKNOWLEDGMENTS

We thank Dr. Yoshiharu Kawaguchi, Department of Embryology, Institute for Developmental Research, Aichi Human Service Center, for providing the HDAC6 antibody used in this study.

REFERENCES

1. Patterson MC, Vanier MT, Suzuki K *et al.* Niemann-Pick disease type C: a cellular cholesterol lipidosis. In: Scriver CR, Beaudet AL, Sly WS, Valle D, eds. *The Metabolic and Molecular Bases of Inherited Disease*, 8th edn. New York: McGraw Hill, 2001; 3611–3634.
2. Vanier MT. Niemann-Pick disease type C. *Orphanet J Rare Dis* 2010; **5**: 16.
3. Suzuki K, Parker CC, Pentchev PG *et al.* Neurofibrillary tangles in Niemann-Pick disease type C. *Acta Neuropathol* 1995; **89**: 227–238.
4. Love S, Bridges LR, Case CP. Neurofibrillary tangles in Niemann-Pick disease type C. *Brain* 1995; **118** (Pt 1): 119–129.
5. Sevin M, Lesca G, Baumann N *et al.* The adult form of Niemann-Pick disease type C. *Brain* 2007; **130**: 120–133.
6. Saito Y, Suzuki K, Hulette CM, Murayama S. Aberrant phosphorylation of alpha-synuclein in human Niemann-Pick type C1 disease. *J Neuropathol Exp Neurol* 2004; **63**: 323–328.
7. Furukawa A, Kawamoto Y, Chiba Y *et al.* Proteomic identification of hippocampal proteins vulnerable to oxidative stress in excitotoxin-induced acute neuronal injury. *Neurobiol Dis* 2011; **43**: 706–714.
8. Inaga S, Katsumoto T, Tanaka K, Kameie T, Nakane H, Naguro T. Platinum blue as an alternative to uranyl acetate for staining in transmission electron microscopy. *Arch Histol Cytol* 2007; **70**: 43–49.
9. Xiong H, Higaki K, Wei CJ *et al.* Genotype/phenotype of 6 Chinese cases with Niemann-Pick disease type C. *Gene* 2012; **498**: 332–335.
10. Kawaguchi Y, Kovacs JJ, McLaurin A, Vance JM, Ito A, Yao TP. The deacetylase HDAC6 regulates aggresome formation and cell viability in response to misfolded protein stress. *Cell* 2003; **115**: 727–738.
11. Kuusisto E, Salminen A, Alafuzoff I. Ubiquitin-binding protein p62 is present in neuronal and glial inclusions in human tauopathies and synucleinopathies. *Neuroreport* 2001; **12**: 2085–2090.
12. Imrie J, Dasgupta S, Besley GT *et al.* The natural history of Niemann-Pick disease type C in the UK. *J Inherit Metab Dis* 2007; **30**: 51–59.
13. Josephs KA, Van Gerpen MW, Van Gerpen JA. Adult onset Niemann-Pick disease type C presenting with psychosis. *J Neurol Neurosurg Psychiatry* 2003; **74**: 528–529.
14. Walterfang M, Fietz M, Fahey M *et al.* The neuropsychiatry of Niemann-Pick type C disease in adulthood. *J Neuropsychiatry Clin Neurosci* 2006; **18**: 158–170.
15. Kumar A, Chugani HT. Niemann-Pick disease type C: unique 2-deoxy-2[(1)(8)F] fluoro-D-glucose PET abnormality. *Pediatr Neurol* 2011; **44**: 57–60.
16. Hulette CM, Earl NL, Anthony DC, Crain BJ. Adult onset Niemann-Pick disease type C presenting with